

Supplementary Information

Opto-Thermophoretic Manipulation of Colloidal Particles in Non-Ionic Liquids

Xiaolei Peng^{1#}, Linhan Lin^{1,2#}, Eric H. Hill^{1,2}, Pranaw Kunal³, Simon M. Humphrey³, and

Yuebing Zheng^{1,2,*}

¹Materials Science & Engineering Program and Texas Materials Institute, The University of Texas at Austin, Austin, TX 78712, USA.

²Department of Mechanical Engineering, The University of Texas at Austin, Austin, TX 78712, USA.

³Department of Chemistry, The University of Texas at Austin, Austin, TX 78712, USA.

*E-mail: zheng@austin.utexas.edu

These authors contributed equally to this work.

Supplementary Videos

Video S1: Trapping and anti-trapping of a 1 μm polystyrene (PS) sphere in water and methanol, respectively. The “+” indicates the laser beam spot.

Video S2: Trapping and anti-trapping of a 2 μm PS sphere in water and methanol, respectively. The “+” indicates the laser beam spot.

Video S3: Release of a 1 μm hydrophilic silica sphere in water when translating it from an optothermal substrate to a glass substrate. The “+” indicates the laser beam spot.

Video S4: Transport and rotation of Ag nanowires (AgNWs) in IPA. The frame rate is 3 times of the original one.

Supplementary Figures

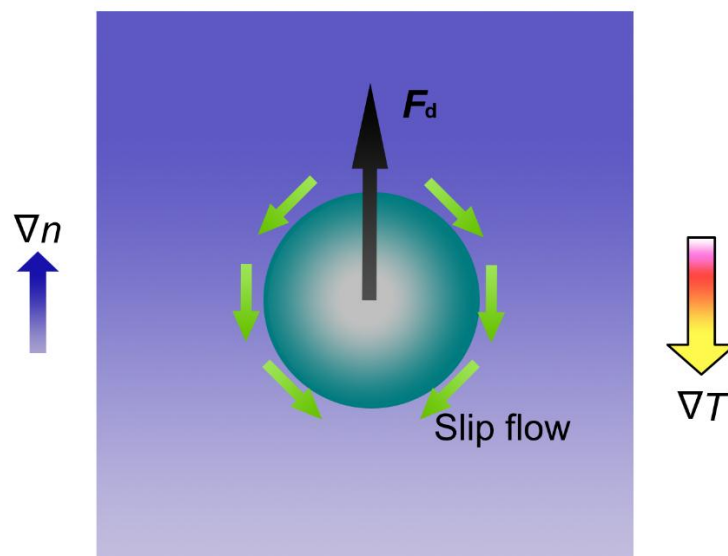


Figure S1: The dispersion force F_d originates from a density gradient of the solvent ∇n induced by the temperature gradient field ∇T . In the particle frame of reference, a slip flow from the cold to hot region occurs at the particle surface. In the laboratory frame of reference, the particle migrates from the hot to the cold region.

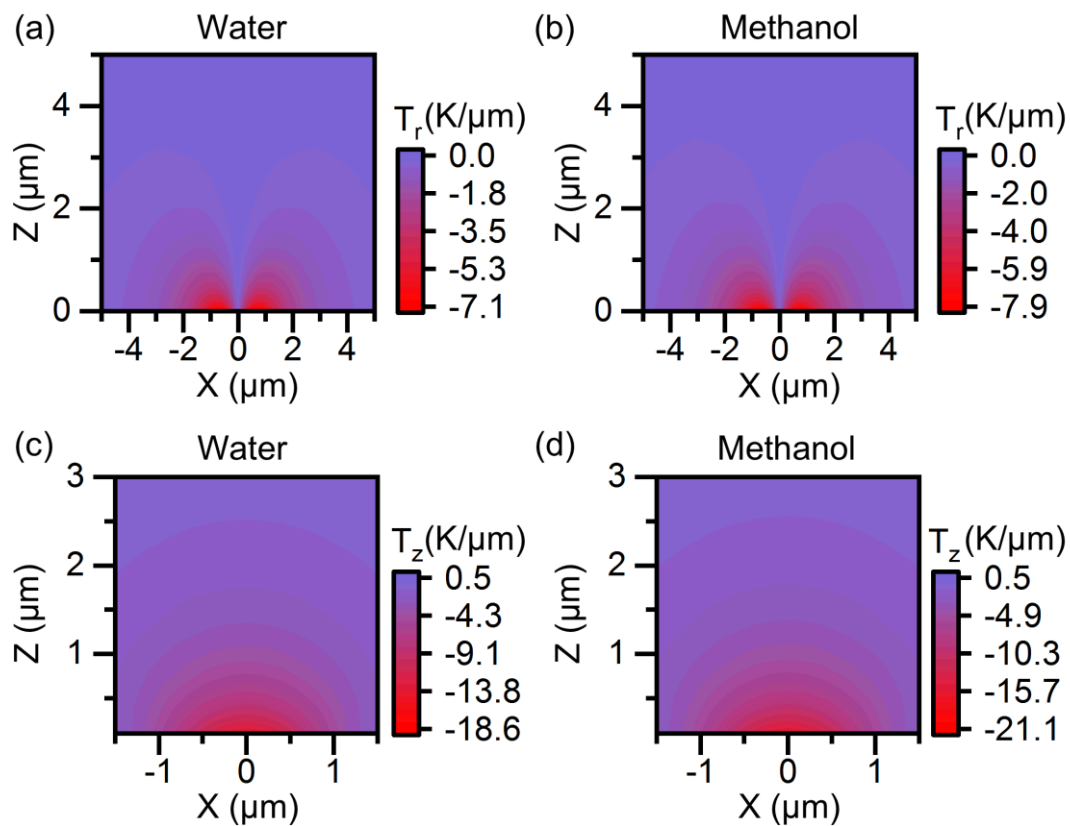


Figure S2: Cross-sectional maps of the temperature gradient field T_r (x-y plane or in-plane) and T_z (z direction) at the substrate-solvent interface where a laser beam with a diameter of $2\ \mu\text{m}$ and a power intensity of $0.16\ \text{mW}/\mu\text{m}^2$ is illuminated onto the substrate beneath a $20\ \mu\text{m}$ thick chamber that contains (a, c) water and (b, d) methanol.

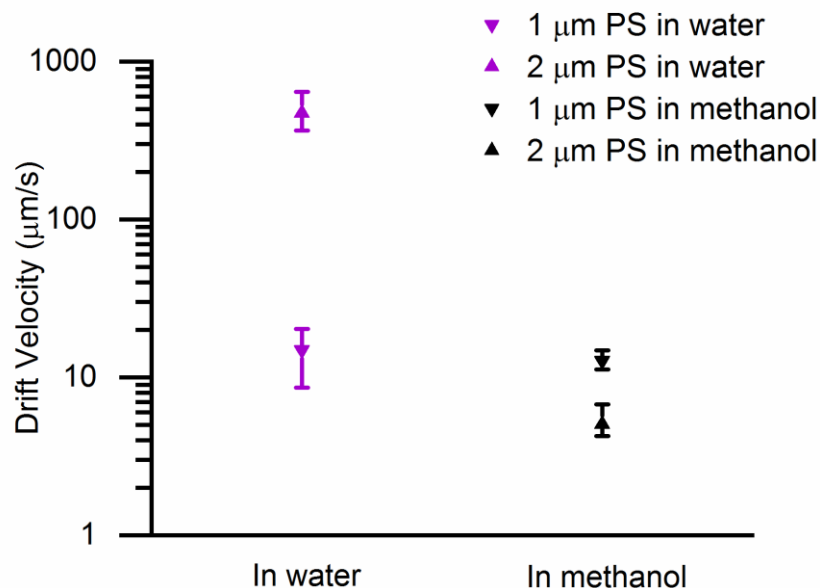


Figure S3: Drift velocities of 1 μm and 2 μm PS particles under a light-generated temperature gradient field in water and methanol. Particles in water drift from the cold to the hot region (*i.e.*, trapping) while particles in methanol drift from the hot to the cold region (*i.e.*, anti-trapping). A laser beam with a diameter of 2 μm and a power intensity of $0.16 \text{ mW}/\mu\text{m}^2$ was focused onto the optothermal substrate to create the localized temperature gradient field.

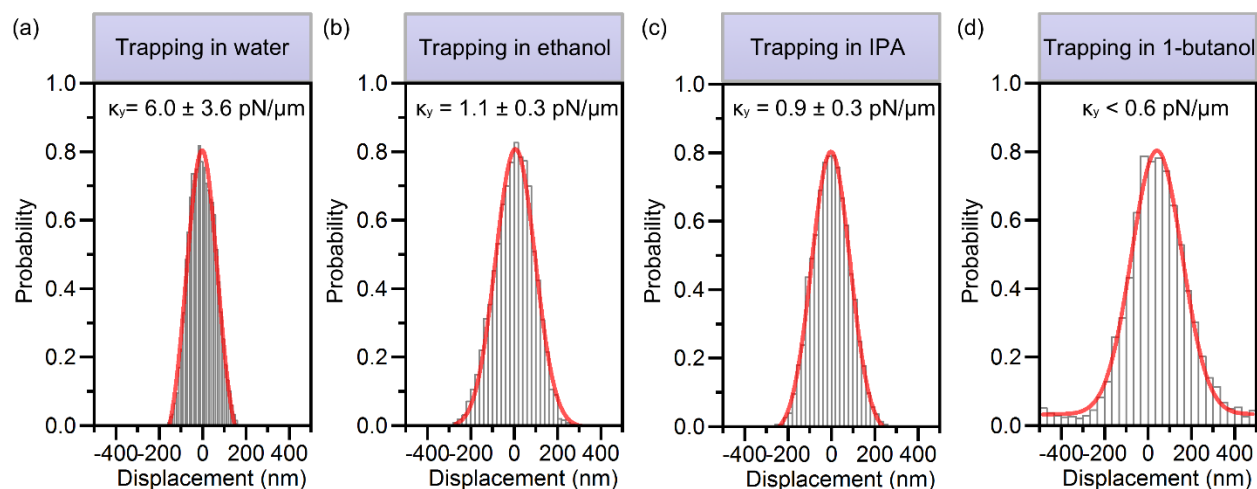


Figure S4: Measured histograms of particle displacement and the corresponding trapping stiffness (y direction) for 500 nm PS spheres under the temperature gradient field in (a) water, (b) ethanol, (c) IPA and (d) 1-butanol.

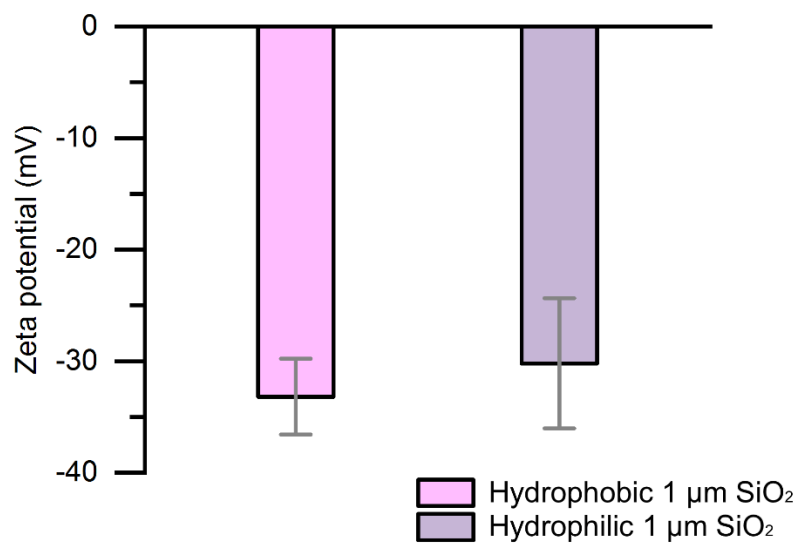


Figure S5: Zeta potentials of 1 μm hydrophobic and hydrophilic silica (SiO_2) particles in water.

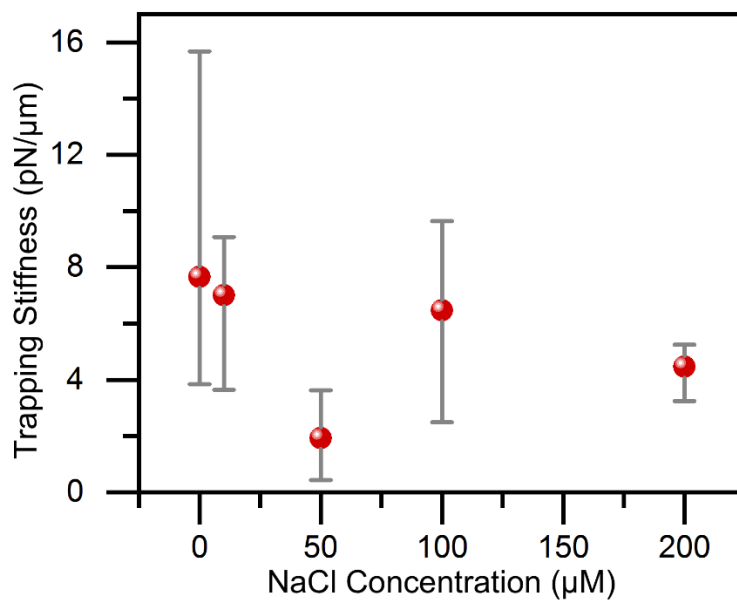


Figure S6: Measured trapping stiffness for 500 nm PS spheres in water as a function of NaCl concentration.

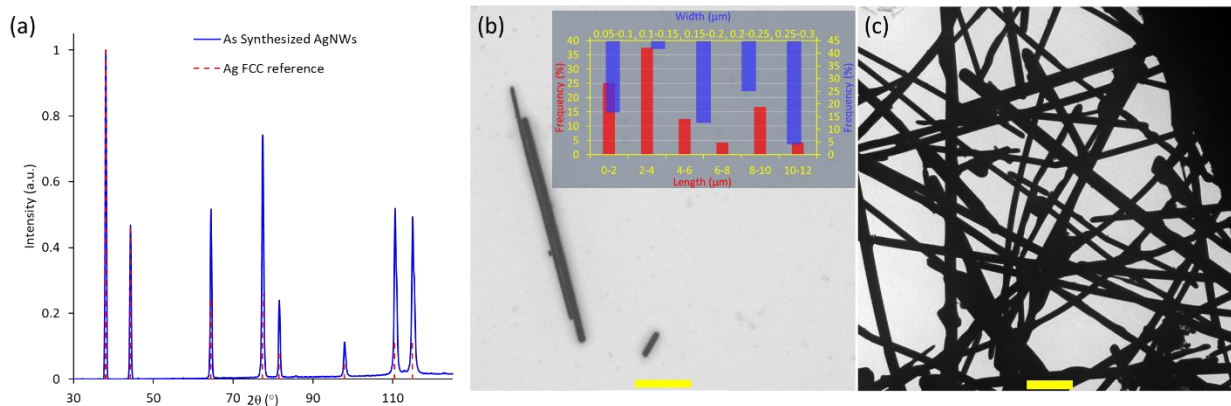


Figure S7: (a) Powder X-ray diffraction spectrum of as-synthesized AgNWs, showing face-centered cubic (FCC) structure. (b-c) Transmission electron micrographs of AgNWs. Inset in (b) shows length (bottom-left axis) and width (top-right axis) distributions of the AgNWs. Scale bars in (b) and (c) are 2 μm and 1 μm , respectively.

Supplementary Table

Table S1. Parameters for calculation of D_T in different solvents at 25 $^{\circ}\text{C}$ (κ_p is 0.03 $\text{W m}^{-1} \text{K}^{-1}$).

Solvents	ϵ_b	η (cP)	κ ($\text{W m}^{-1} \text{K}^{-1}$)	$\frac{\epsilon_b}{\eta T} \frac{2\kappa}{2\kappa + \kappa_p}$ ($\text{cP}^{-1} \cdot \text{K}^{-1}$)
Water	78.5	1.082	0.606	0.118
Methanol	31.5	0.545	0.198	0.090
Ethanol	24.3	0.890	0.159	0.042
IPA	18.0	1.960	0.136	0.014
1-butanol	17.3	2.544	0.155	0.011